Geomechanics and Engineering, *Vol. 20, No. 4 (2020) 313-322*
DOI: https://doi.org/10.12989/gae.2020.20.4.313

An improved approach to evaluate the compaction compensation grouting efficiency in sandy soils

Xiang-Hua Xu[2], Zhou-Chen Xiang[1], Jin-Feng Zou*[1] and Feng Wang[1]

[1]School of Civil Engineering, Central South University, No.22, Shaoshan South Road, Central South University Railway Campus, Changsha, Hunan Province, People's Republic of China
[2]Guizhou Provincial Communications Department, No. 66, Yan'an West Road, Guiyang, Guizhou Province, People's Republic of China

(Received January 11, 2019, Revised January 13, 2020, Accepted February 2, 2020)

Abstract. This study focuses on a prediction approach of compaction compensation grouting efficiency in sandy soil. Based on Darcy's law, assuming that the grouting volume is equal to the volume of the compressed soil, a two-dimensional calculation model of the compaction compensation grouting efficiency was improved to three-dimensional, which established a dynamic relationship between the radius of the grout body and the grouting time. The effectiveness of this approach was verified by finite element analysis. The calculation results show that the grouting efficiency decreases with time and tends to be stable. Meanwhile, it also indicates that the decrease of grouting efficiency mainly occurs in the process of grouting and will continue to decline in a short time after the completion of grouting. The prediction three-dimensional model proposed in this paper effectively complements the dynamic relationship between grouting compaction radius and grouting time, which can more accurately evaluate the grouting efficiency. It is practically significant to ensure construction safety, control grouting process, and reduce the settlement induced by tunnel excavation.

Keywords: compensation grouting; grouting efficiency; filtration; sandy soils; soil settlement

1. Introduction

Compaction grouting technique has been widely used to enforce soft foundation, surrounding rock, tunnel face, pile, correction of building, subgrade subsidence, etc. (Chen *et al.* (2015), Ibrahim *et al.* (2015), Zhang *et al.* (2015), Bellendir E N *et al.* (2016), Merkin Valery *et al.* (2016), Zheng and Zuo (2017), Pan *et al.* (2017), Ukritchon *et al.* (2017), Stark Alfred *et al.* (2017), Dan *et al.* (2017), Zou *et al.* (2017), Dan *et al.* (2018), Pan *et al.* (2018), Zou *et al.* (2018), Bing B R *et al.* (2018), Huang *et al.* (2019), Li and Zou (2019), Zou *et al.* (2019a), Chen *et al.* (2019a), Zou *et al.* (2019b), Zou *et al.* (2019c), Zou and Zhang (2019), Chen *et al.* (2019b), Chen *et al.* (2019c), Li *et al.* (2020), Li and Yang (2020), Qian *et al.* (2020), Zou *et al.* (2020), Zou and Wei (2020)). When the purpose of grouting is to compensate for surface settlement induced by tunnel excavation, it can be called as compensation grouting. Generally, the grout is injected into the part between the tunnel excavation area and the building to compensate for volume loss caused by excavation, which is aimed at reducing ground settlement.

Meanwhile, in recent years, many scholars have carried out research on evaluating grouting efficiency. Zheng *et al.* (2017), based on the extension theory, introduced a feasible and scientific method to evaluate the grouting effects of water-rich fault in tunnels systematically. Kim and Park (2017), according to results of grouting tests, evaluated the improved strength of the ground by applying the bio grouting method to a loose sandy ground. Lee *et al.* (2017) investigate the factors affecting waterproof efficiency of grouting in single rock fracture through laboratory experiments. Fan *et al.* (2016) proposes a hybrid fuzzy comprehensive evaluation method to assess curtain grouting efficiency by considering both the permeability and tightness of a grout curtain. As for compaction compensation grouting, the efficiency of it, which can be used to evaluate compensation grouting effect, is defined as the ratio of uplift volume to total grouting volume. In ideal state, the compensation grouting efficiency will be equal to 1, but due to pressure filtration, the fine particles and water in the grout will be transferred into the surrounding soil, resulting in the decrease of grouting efficiency. At present, although some scholars have done some theoretical research on compensation grouting efficiency, they still mainly focus on experimental methods.

The variation tendency and calculation methods of compensation grouting efficiency are different in different soil types. In clayed soils, as the low permeability hinders the progress of the permeation, the compensation grouting efficiency is close to 1. Due to the consolidation, there are some difficulties in obtaining a specific grouting efficiency calculation method. Field tests by and Au *et al.* (2003) showed that the compensation grouting efficiency was only 3 to 22%. Au *et al.* (2001) and Soga (2004) observed through experiments that in normal consolidated clay, the grouting efficiency value was about 80-90% after the

*Corresponding author, Professor
E-mail: zoujinfeng_csu@163.com

ISSN: 2005-307X (Print), 2092-6219 (Online)

completion of grouting, but then it would keep decreasing. Au *et al.* (2003) researched the influencing factors of compensation grouting efficiency in clay and compared the experimental data with the numerical simulation results, showing that the grouting efficiency decreased significantly with time. Furthermore, it was observed that the efficiency increased with the increase of OCR and the decrease of water-cement ratio of the grout. In silty soils, there are some difficulties in evaluating the grouting efficiency due to grout permeation and soil compaction. Although Masini (2010) and Masini *et al.* (2011) obtained a relatively low value of compensation grouting efficiency (26%) through experiments, but no specific theoretical method has yet been found to prove the cause of this phenomenon. In sandy soils, to research the effect of water-cement ratio (w/c), bentonite content (b.c.) and injection rate on the compensation grouting efficiency, Soga *et al.* (2012) conducted two physical model experiments of compensation grouting in sand with two different setups (Cambridge setup and Delft setup), showing that the compensation efficiency greatly reduced with the decrease of soil density. On this basis, Luca Masini *et al.* (2014) proposed a specific formula based on Darcy's law to calculate the compensation grouting efficiency in sandy soils. However, the influence of the grout bulb radius increasing in the grouting process on the grouting efficiency was not considered in his calculation.

In short, the current research on grouting efficiency is mainly focused on experimental methods. Based on Luca Masini's *et al.* (2014) approach, a three-dimensional improved model was proposed in this paper. Regarding the radius of the grouting body as a function related to time, the dynamic relationship between grouting efficiency and grouting time was emphatically researched.

2. Methodology

2.1 Problem definition

2.1.1 Pressure filtration model

Au *et al.* (2002) proposed that the compensation grouting efficiency can be defined as

$$\xi = \frac{V_{SH}}{V_{inj}} \tag{1}$$

where V_{SH}= volume of heave induced at the ground surface by the injection process; and V_{inj} = volume of injected grout. In sandy soils, some scholars have proposed corresponding calculation formulas to evaluate the compensation grouting efficiency. Grouting efficiency ξ can be defined as

$$\xi = \frac{V_{SH}}{V_S}\frac{V_S}{V_{GB}}\frac{V_{GB}}{V_{inj}} = \eta_G \eta_S \eta_F \tag{2}$$

where $\eta_G=V_{SH}/V_S$ (the geometry effect); $\eta_S=V_S/V_{GB}$ (the soil compaction/consolidation); $\eta_F=V_{GB}/V_{inj}$ (the grout filtration effect); V_{GB}=final volume of the grout body; and V_S=increased soil volume due to grouting.

Soga *et al.* (2004) noted that the increased volume of the grout body should be equal to the injected volume in ideal conditions, so that the grouting efficiency was equal to 1. However, the truth is quite different. Experimental studies (Bezuijen *et al.* 2007, Gustin *et al.* 2007, Sanders *et al.* 2007) showed that some fine particles and water would filtrate from the grout body into the soil due to the pressure filtration, resulting in that the increased volume was always less than the volume of injected grout. In sandy soils, solid particles clog the sand pore closely around the injection body, which prevent further solids permeation. Therefore, it can be assumed that the majority of the filtration is water during the pressure filtration, and then the calculation of grouting efficiency can be simplified as

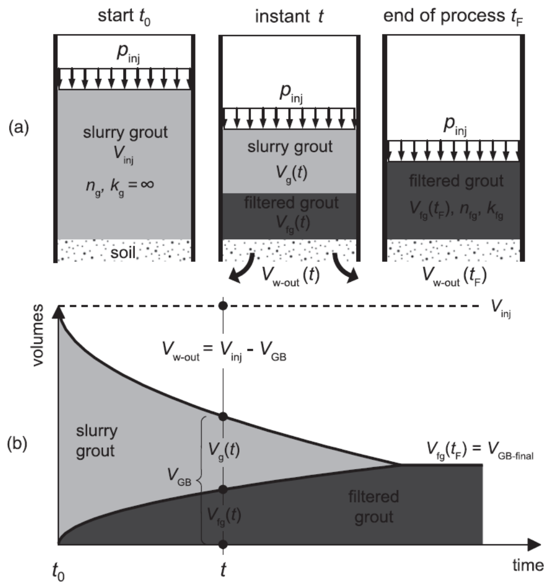

Fig. 1 Pressure filtration and particle accumulation: (a) one dimensional model and (b) volume changes with time (adapted from Masini *et al.* (2014))

$$\xi = \eta_F = \frac{V_{GB}}{V_{inj}} = \frac{V_{inj} - V_{w-out}}{V_{inj}} = 1 - \frac{V_{w-out}}{V_{inj}} \tag{3}$$

where V_{w-out} is the volume of fluid lost by pressure filtration. Generally, V_{w-out} increases with increasing permeability of soil, causing grouting efficiency to decrease.

On this basis, Luca Masini *et al.* (2014) proposed an approach to calculate the compensation grouting efficiency. The pressure filtration process for compensation grouting is shown in Fig.1. If a grouting pressure p_{inj} is applied to the initial slurry grout body with porosity n_g, a part of the water will permeate into the soil from the grout. Finally, a region will be formed between the grout and the soil by accumulation of coarse grout particles, called filtered grout. In this process, the volume of the slurry grout $V_{G(t)}$ decreases with time, while the volume of the filtered slurry $V_{fg(t)}$ keeps increasing continuously. Until the end, $t=t_f$, all excess water seeps out of the slurry grout and then the whole slurry grout becomes the filtered grout.

If the slurry grout solidifies completely and turns into filtered grout, the total volume of water flowing out of the

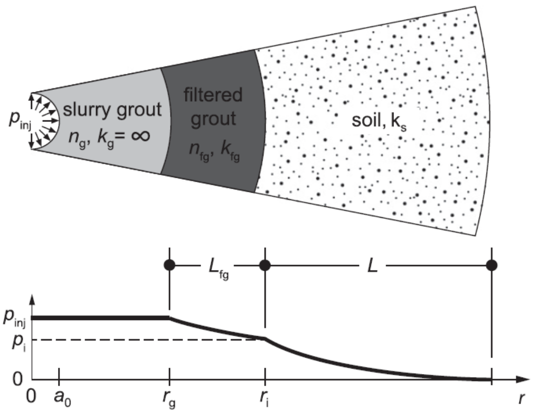

Fig. 2 Spherical model of grouting and pressure filtration (adapted from Masini *et al.* (2014))

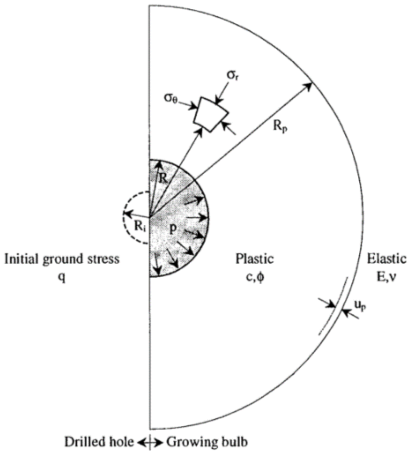

Fig. 3 Grouth of grout bulb (adapted from El-Kelesh *et al.* (2001))

slurry grout is as follows:

$$V_{w-out} = \frac{n_g - n_{fg}}{1 - n_g} V_{fg} \tag{4}$$

where n_g and n_{fg} are porosity of soil and permeable layer respectively.

Derivation of time on both sides of Eq. (4) is as follows:

$$\frac{dV_{w-out}}{dt} = \frac{n_g - n_{fg}}{1 - n_g} \frac{dV_{fg}}{dt} \tag{5}$$

The spherical model of the grouting process is shown in Fig. 2. With constant injection rate q_{inj}, the grout body expands spherically from initial radius a_0. And when grouting time reaches t, the radius of grout body will increase to r_i and the thickness of filtered grout will increase to L_{fg} when time is t. According to the mass conservation and Darcy's law, the flow rate of pore water moving outward in the filtered grout can be written as follows:

$$Q = \frac{dV_{w-out}}{dt} = -k \frac{dp}{dr} \frac{1}{\gamma_w} 4\pi r^2 \tag{6}$$

where γ_w is unit weight of water, r is the distance where pore pressure can be negligible and k is permeability coefficient.

Assuming that the flow of water passing through the filtered grout is equal to the flow entering into the soil, integrate the Eq. (6) and the grout pressure p_{inj} can be obtained,

$$p_{inj} = \frac{Q}{4\pi} \gamma_w \left[\frac{1}{k_{fg}} \left(\frac{1}{r_i} \right)_{r_i}^{r_i - L_{fg}} + \frac{1}{k_s} \left(\frac{1}{r_i} \right)_{r_i + L}^{r_i} \right] \tag{7}$$

where L=r-r_i, r_i is the radius of the grout body at time t, and k_s and k_{fg} are the permeability coefficient of soil and the filtered grout respectively

By Eq. (5) and Eq. (6)

$$Q = \frac{dV_{w-out}}{dt} = \frac{n_g - n_{fg}}{1 - n_g} \frac{dV_{fg}}{dt} = 4\pi \frac{n_g - n_{fg}}{1 - n_g} \left(r_i - L_{fg} \right)^2 \frac{dL_{fg}}{dt} \tag{8}$$

and substituting Eq. (8) into Eq. (7)

$$\frac{dL_{fg}}{dt} = \frac{1 - n_g}{n_g - n_{fg}} \frac{p_{inj}}{\gamma_w} \frac{1}{\left(r_i - L_{fg} \right)^2} \left[\frac{L_{fg}}{k_{fg} r_i \left(r_i - L_{fg} \right)} + \frac{L}{k_s r_i \left(r_i + L \right)} \right]^{-1} \tag{9}$$

where L_{fg} and r_i are related to time t, whereas the remaining quantities are constants. And dL_{fg}/dt can be derived from Eq. (9) and grouting efficiency η_F can be obtained.

The calculation method of grouting efficiency proposed by Luca Masini *et al.* (2014) actually uses the volume of water flowing into the soil from the grout to replace the reduced volume of the grout in the soil, which is reasonable under the assumption. However, Luca Masini *et al.* (2014) noted in the paper that r_i is related to time, but in the derivation, r_i was treated as a constant. In the actual grouting process, from the initial moment, r_i varies with time, injection pressure and the physical properties of the grout and soil. It means, during the grouting process, the pressure filtration and the grout bulb expansion occur simultaneously.

2.1.2 Cavity expansion model

Generally, the compaction grout bulb is modeled as an expanding spherical cavity in an isotropic elastic-plastic continuum. The surrounding soil behaves elastically until the onset of yield, which is determined by Mohr-Coulomb criterion. At the start of injection, the radius of the bulb, or cavity, is the drilling radius a_0. With grout injection, the grout bulb radius expands in all the directions to r_i and a spherical zone of radius R_p around the grout bulb pass into the state of plastic equilibrium (grouth of grout bulb is shown as follows). Beyond the elastoplastic interface, the soil remains in a state of elastic equilibrium.

El-Kelesh *et al.* (2001) proposed a method for calculating the radius of grout body in compacting grouting. He indicated that at a certain depth, every suitable grouting pressure corresponds to a plastic zone radius and an extreme bulb radius. It means that the grout bulb radius will increase from the initial radius a_0 to the ultimate radius R_u. Once R_u is attained, the grout will be difficult to be injected into soil, which leads the grout bulb will not expand further.

The calculation formula is as follows:

$$R_u = \frac{a_0}{\left[a_1\left(\frac{p_{inj}+a_2}{a_3}\right)^{a_4} + \left(\frac{a_3}{p_{inj}+a_2}\right)^{a_4} - a_5\right]^{\frac{1}{3}}} \tag{10}$$

where

$$a_1 = \frac{1}{I_r} - 1 + \left(1 - \frac{1+\nu}{2E}\frac{4\sin\varphi}{3-\sin\varphi}\left(q + c\cos\varphi\right)\right)^3 \tag{11}$$

$$a_2 = c\cot\varphi \tag{12}$$

$$a_3 = \frac{3\left(1+\sin\varphi\right)}{3-\sin\varphi}\left(q + c\cot\varphi\right) \tag{13}$$

$$a_4 = \frac{3\left(1+\sin\varphi\right)}{4\sin\varphi} \tag{14}$$

$$a_5 = \frac{1}{I_r} \tag{15}$$

a_0 is the drilling radius or initial cavity radius, a_1, a_2, a_3, a_4, and a_5 are constants depending on the soil type and injection depth, q is initial isotropic ground stress and I_r is the stiffness coefficient which represents the ratio of shear modulus to initial shear strength,

$$I_r = \frac{G}{S} = \frac{E}{2\left(1+\nu\right)\left(c + q\tan\varphi\right)} \tag{16}$$

In combination with Luca Masini's model and Adel M. El-Kelesh' thoeries, the pressure filtration process of the grout can be divided into two Stages during the whole grouting process. In the first Stage, the grout body radius r_i keeps expanding from a_0, meanwhile the filtration occurs and the water in the slurry grout permeate into surrounding soil, with the increasing of the filtered grout thickness. In the second Stage, when the grout body radius has reached R_u, calculated by Eq. (10), the injection will be stopped and the grout body radius will no longer increase. But L_{fg} will continue to increase until the filtration in the slurry grout is finished completely.

2.2 Assumptions

In order to simplify the calculation model, the following assumptions is proposed in this paper:

- Bezuijen (2008) noted that compensation grouting can be considered as a process accompanied by compaction grouting and fracture grouting. Because the shape of grout body in facture grouting can't be determined specifically, for the convenience of calculation, the compensation grouting is treated as compaction grouting and the grout body is assumed to be spherically diffused in the soil.
- In sandy soils, as pressure filtration develops and water flows out from the grout, the grout body volume expands but is smaller than the injected volume. The injected volume is equal to the sum of the lost water volume and the expanding volume, which can be described as follows,

$$q_{inj}t - V_{w-out} = \frac{4\pi}{3}r_i^3 \tag{17}$$

Then

$$r_i = \sqrt[3]{\frac{3}{4\pi}\left(q_{inj}t - V_{w-out}\right)} \tag{18}$$

In the proposed improved model, the calculation of V_{w-out} should depend on r_i. Bring Eq. (18) into this model, the equation cannot be solved. Considering the sandy soils has good permeability, the water in grout will be lost in a short time after injection. For the convenience of calculation, it is assumed that,

$$\eta_{F(\min)}q_{inj}t = \frac{4\pi}{3}r_i^3 \tag{19}$$

$$\eta_{F(\min)} = \frac{V_{GB-final}}{V_{inj}} = \frac{1-n_g}{1-n_{fg}} \tag{20}$$

where $\eta_{F(min)}$ is the minimum grouting efficiency and $V_{GB-final}$ is final volume of the grout body.

Then

$$r_i = \sqrt[3]{\eta_{F(\min)}\frac{3}{4\pi}q_{inj}t} \tag{21}$$

- During the pressure filtration, it is assumed that only water permeates into soil while solid particles do not permeate.
- In the grouting process, the variation of some parameters such as porosity and permeability coefficient caused by soil compression is not be considered. It is assumed that these parameters are constant value.
- The self-weight effect is negligible.
- The slurry grout and the filtered grout remain fully saturated

2.3 Solutions

Stage I

r_i and L_{fg} vary with time t and dV_{fg1}/dt in Eq. (5) can be expressed as follows:

$$\frac{dV_{fg1}}{dt} = \frac{d\frac{4\pi}{3}\left[r_i^3 - \left(r_i - L_{fg}\right)^3\right]}{dt} = \frac{4\pi}{3}\left(\frac{dr_i^3}{dt} - \frac{d\left(r_i - L_{fg}\right)^3}{dt}\right) \tag{22}$$

and then Q can be expressed as follows:

$$Q_1 = \frac{dV_{w-out1}}{dt} = \frac{n_g - n_{fg}}{1-n_g}\frac{dV_{fg1}}{dt} \tag{23}$$

where

$$\frac{dr_i^3}{dt} = 3r_i^2\left(\eta_{F(\min)}q_{inj}t\frac{3}{4\pi}\right)^{-\frac{2}{3}}\frac{1}{4\pi}\eta_{F(\min)}q_{inj} \tag{24}$$

$$\frac{d\left(r_i-L_{fg}\right)^3}{dt}=3\left(r_i-L_{fg}\right)^2\left(\frac{dr_i}{dt}-\frac{dL_{fg}}{dt}\right) \tag{25}$$

$$\frac{dr_i}{dt}=\left(\eta_{F(\min)}q_{inj}t\frac{3}{4\pi}\right)^{-\frac{2}{3}}\frac{1}{4\pi}\eta_{F(\min)}q_{inj} \tag{26}$$

Eq. (7) can be replaced as

$$p_{inj}=\frac{Q_1}{4\pi}\gamma_w\left[\frac{1}{k_{fg}}\left(\frac{L_{fg1}}{r_i\left(r_i-L_{fg1}\right)}\right)+\frac{1}{k_s}\left(\frac{L}{r_i\left(r_i+L\right)}\right)\right] \tag{27}$$

where r_i is expressed by Eq. (21). Luca Masini *et al.* (2014) noted that L=2ri in real condition. Substituting them into Eq.(27)

$$p_{inj}=\frac{Q_1}{4\pi}\gamma_w\left[\frac{1}{k_{fg}}\left(\frac{L_{fg1}}{r_i\left(r_i-L_{fg1}\right)}\right)+\frac{1}{k_s}\left(\frac{2}{3r_i}\right)\right] \tag{28}$$

and the thickness of filtered grout L_{fg1} can be figured out.

The volume of filtered grout in this stage is

$$V_{fg1}=\left[r_i^3-(r_i-L_{fg1})^3\right]\cdot\frac{4}{3}\pi \tag{29}$$

Substituting Eq. (29) into Eq. (3), the grouting efficiency in this stage can be calculated as follows:

$$\eta_{F1}=1-\frac{\frac{4\pi}{3}\cdot\frac{n_g-n_{fg}}{1-n_g}\cdot\left[r_i^3-(r_i-L_{fg1})^3\right]}{q_{inj}t} \tag{30}$$

where r_i can be substituted by Eq. (21).

Stage II

In the grouting process, r_i keeps increasing until r_i=R_u and then it will be equal to the constant R_u. But at this time, the pressure filtration of grout has not finished. L_{fg} will keep increasing with time. This stage starts at t_0, which can be got by Eq. (19) and Eq. (21) as

$$t_0=\frac{4\pi R_u^3}{3q_{inj}\eta_{F(\min)}} \tag{31}$$

where R_u is calculated by Eq. (10).

From t_0, dV_{fg}/dt in Eq. (5) can be expressed as

$$\frac{dV_{fg2}}{dt}=4\pi\left(R_u-L_{fg}\right)^2\frac{dL_{fg2}}{dt} \tag{32}$$

and then Q can be expressed as

$$Q_2=\frac{dV_{w-out2}}{dt}=\frac{n_g-n_{fg}}{1-n_g}\frac{dV_{fg2}}{dt}=4\pi\frac{n_g-n_{fg}}{1-n_g}\left(R_u-L_{fg}\right)^2\frac{dL_{fg2}}{dt} \tag{33}$$

$$p_{inj}=\frac{Q_2}{4\pi}\gamma_w\left[\frac{1}{k_{fg}}\left(\frac{L_{fg2}}{R_u\left(R_u-L_{fg2}\right)}\right)+\frac{1}{k_s}\frac{2}{3R_u}\right] \tag{34}$$

and substituting Eq. (22) into Eq. (23)

$$\frac{dL_{fg2}}{dt}=\frac{1-n_g}{n_g-n_{fg}}\frac{p_{inj}}{\gamma_w}\frac{1}{\left(R_u-L_{fg2}\right)^2}\left[\frac{L_{fg2}}{k_{fg}R_u\left(R_u-L_{fg2}\right)}+\frac{2}{3k_sR_u}\right]^{-1} \tag{35}$$

And then the thickness of filtered grout L_{fg2} can be figured out by substituting Eq. (34) into Eq. (35).

The volume of filtered grout in this stage is

$$V_{fg2}=\left[R_u^{\ 3}-(R_u-L_{fg2})^3\right]\cdot\frac{4}{3}\pi \tag{36}$$

Substituting Eq. (3) and Eq. (4) into Eq. (22), the grouting efficiency in this stage can be calculated as follows:

$$\eta_{F2}=1-\frac{\frac{4\pi}{3}\cdot\frac{n_g-n_{fg}}{1-n_g}\cdot\left[R_u^{\ 3}-(R_u-L_{fg1})^3\right]}{R_u^{\ 3}} \tag{37}$$

3. Numerical simulation of the theoretical model

Luca Masini *et al.* (2014) has done a model test and attained some data of grouting efficiency, but the model is 1D while the proposed approach is 3D, which will make some severe differences in results comparison. Due to the lack of other relevant data, finite element analysis is used to verify the calculation result.

The calculation parameters are shown in Table 1, selected from El-Kelesh *et al.* (2001) and Luca Masini *et al.* (2014).

It can be attained that R_u=0.4423m and t_0=1118s. It means that, with above parameters, the maximum radius of

Table 1 Related material parameters

Unit weight of soil $\gamma_s(kg/m^3)$	Deformation modulus $E(MPa)$	Cohesion of soil $c(MPa)$	Friction angle $\varphi(^o)$
16	981.645	0	34.6
injection pressure $p_{inj}(kPa)$	injection rate $q_{inj}(m^3/s)$	initial radius $a_0(m)$	Permeability of soil $k_s(m/s)$
1200	4×10^{-4}	0.025	4.9×10^{-7}
permeability of the filtered grout k_{fg}=2.5×10^{-7}	porosity of the slurry grout n_g	porosity of the filtered grout n_{fg}	Poisson ratio ν
	0.597	0.522	0.3

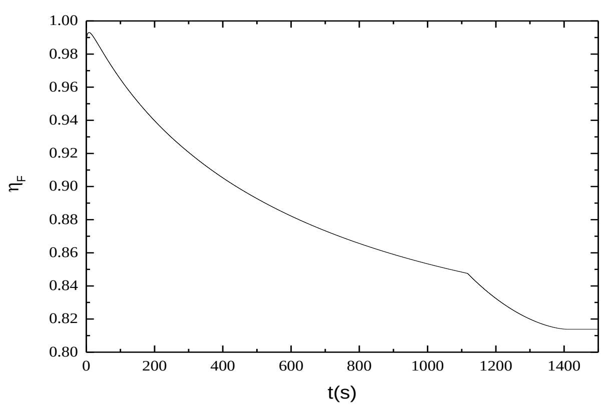

Fig. 4 The graph of η_F related to t

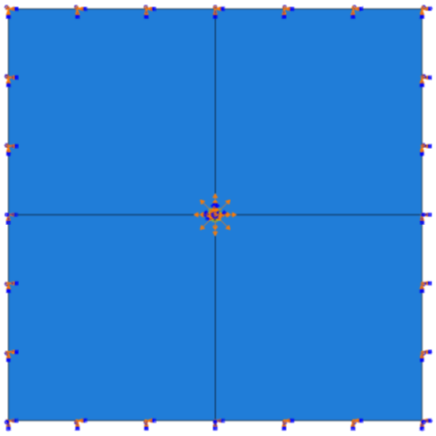

Fig. 5 Boundary conditions

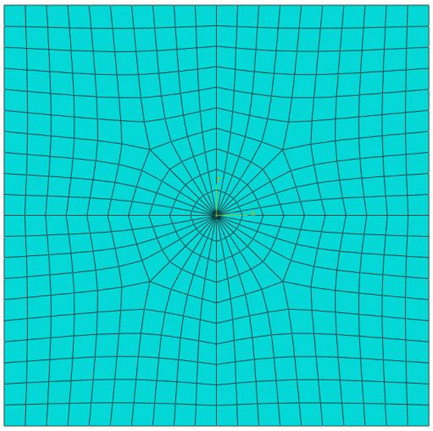

Fig. 6 Profile of the finite-element mesh

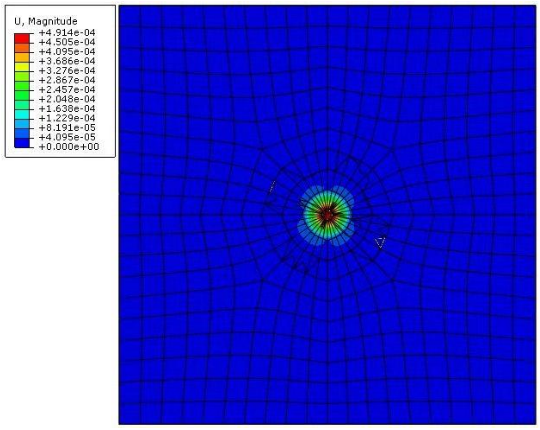

Fig. 7 The displacement at initial time

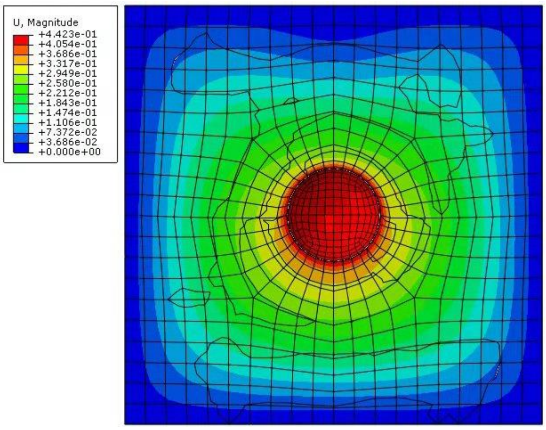

Fig. 8 The displacement at ending time

grout body is about 0.4423 meters and it takes about 1118 seconds to reach this value from the beginning. Therefore, ***Stage I*** is 0 to 1118 seconds and ***Stage II*** is 1118 seconds to the end when pressure filtration is finished.

The thickness of filtered grout L_{fg} and the grouting efficiency η_F in two stages can be calculated after the Ru and t0 have been figured out. The graph of η_F varying with time is shown in Fig. 4.

In the proposed approach, compensation grouting process is divided into two Stages. In ***Stage I***, the grout body keeps expanding and the water is flowing into soil from the grout. In ***Stage II***, the grout body will no longer increase but the pressure filtration is still going on. Therefore, ***Stage II*** can be considered as the complex form of ***Stage I***, as their mechanism is the same. And if the rationality of ***StageI*** has been verified, the verification of ***Stage II*** will not need to be done. Thus, only ***Stage I*** need to be verified.

ABAQUS 6.14 is used to simulate the grouting and pressure filtration process.

In the numerical analysis, a sphere cavity with radius of 0.025 m is set in the center of cubic soil body (4 m×4 m×4 m in length × width × thickness). The six faces of the model are completely fixed and a pore pressure boundary condition (magnitude is equal to the injection pressure p_{inj}) is set on the face of sphere hole. And the outer faces and the inner face were set to be drained. Additionally, on the inner surface, a radial displacement boundary condition (magnitude is 0.4423 m) with linear variation is adopted to simulate the process of grout propagation into the soil. The boundary condition of the model is shown in Fig. 5. The time of the analysis step is set from 0 to 1118 s, which is the time of ***Stage I***. The mesh size was set as 0.2m on the soil boundary and the mesh size on the inner sphere surface is set as 0.01m, as shown in Fig. 6. And the model is made of 9024 linear hexahedral elements of type C3D8P. The material parameters in Table 1 are used in this finite-element model.

The profiles of cavity expansion at initial time and ending time are shown in Figs. 7 and 8, respectively.

Taylor (1984) proposed that, in sandy soils, there is a relationship between permeability coefficient and void ratio as follows:

$$k_1 : k_2 = e_1^2 : e_2^2 \tag{38}$$

The permeability coefficient can be set to vary with the void ratio in *ABAQUS*. Therefore, the relation curve of k and e has been set in the model according to Eq. (38). Then the volume of fluid lost by pressure filtration ($V_{w\text{-}out}$) can be got and the grouting efficiency η_F has been figured out by Eq. (3). Fig. 9 shows the results comparison of the F.E. analysis and the proposed approach.

In the proposed approach, the variation of the void ratio and the permeability coefficient of soil caused by

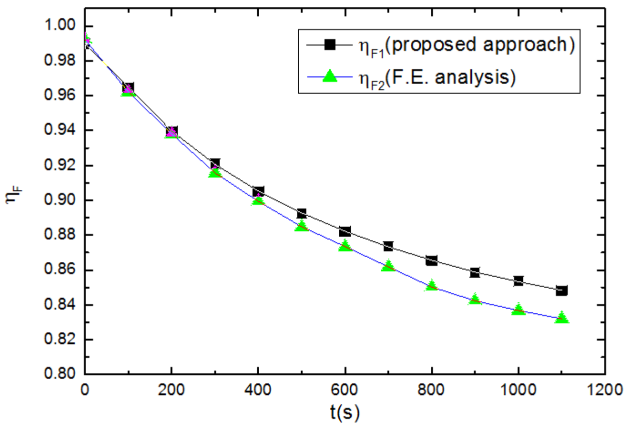

Fig. 9 The comparison of results between F.E. analysis and proposed approach

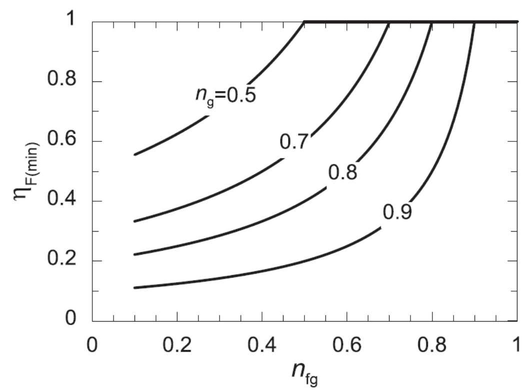

Fig. 10 The relationship of $\eta_{F(min)}$, n_g and n_{fg}

compaction is not considered. In the F.E. analysis, it is difficult to simulate the complete injection process and the analysis is carried out by considering the variation of the void ratio and the permeability coefficient. There may be some deviations in the two ways. From the comparison in Fig. 9, it can be observed that the variation trends of the two ways are close and the most deviation is about only ±3%, which is acceptable. Therefore, the effectiveness of the proposed approach is validated.

4. Parameters analysis

In the model of pressure filtration described previously, the maximum grouting radius of compaction grouting will remain invariable when γ_s, φ, E, c, p_{inj} and v are constants. And then the following factors can affect the thickness of filtered grout and the grouting efficiency:

- Injection pressure p_{inj} and injection rate q_{inj}.
- Slurry grout porosity n_g and filtered grout porosity n_{fg}.
- Soil permeability coefficient k_s and filtered grout permeability coefficient k_{fg}.

Luca Masini *et al.* (2014) proposed that n_g was determined by the content of cement and bentonite, n_{fg} and k_{fg} were determined by grout physical property (Water-cement ratio w/c and bentonite-water ratio b/w) and injection process, and p_{inj} was the key factor affecting n_{fg} and k_{fg}. The relationship of ng and n_{fg} is as follows:

$$\frac{n_{fg}}{n_g} = \frac{1}{a\left(\frac{p_{inj}}{p_a}\right)^b + 1} \tag{39}$$

where p_a is the atmosphere pressure, and a and b are the coefficient related to w/c, providing $n_g = n_{fg}$ for $p_{inj}/p_a=0$

4.1 n_g and n_{fg}

From Eq. (20), it can be observed that the final grouting efficiency $\eta_{F(min)}$ is only related to ng and n_{fg}, showing in Fig. 10.

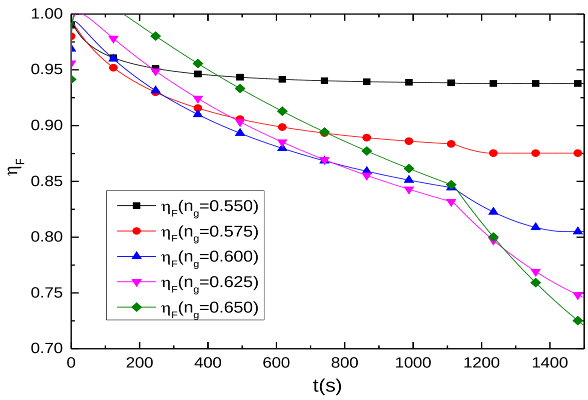

Fig. 11 The influence of n_g on η_F when n_{fg}=0.522

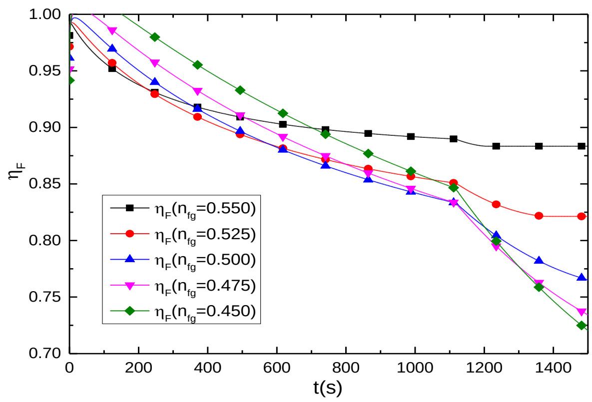

Fig. 12 The influence of n_{fg} on η_F when n_g=0.597

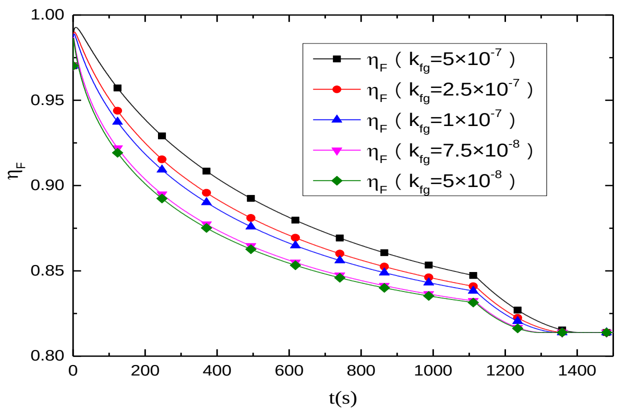

Fig. 13 The influence of k_s on η_F when k_{fg}=2.5×10^{-7}m/s

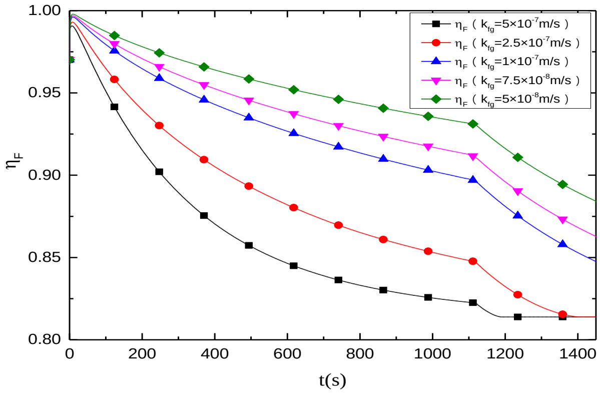

Fig. 14 The influence of k_{fg} on η_F when k_s=4.9×10^{-7}m/s

The graphs of η_F varying with n_g and n_{fg} are shown in Figs. 11 and 12, respectively.

Based on the calculation results, it can be observed that the final magnitude of η_F and its variation are determined by n_g and n_{fg} directly. The process of the pressure filtration will be longer with the increasing n_g and the decreasing n_{fg}. It means that the more magnitude of n_g/n_{fg}, the slower process of the pressure filtration.

4.2 k_s and k_{fg}

η_F is also affected by k_s and k_{fg}. The graphs of η_F varying with k_s and k_{fg} are shown in Figs.13 and14.

Based on the calculation results, it can be observed that the pressure filtration is mainly affected by k_{fg} and the variation of k_s has little effect on the process of pressure infiltration.

5. Conclusions

In this paper, based on Darcy's law, regarding the radius of grout body in the grouting process as a function related to time, an improved approach to evaluate the compensation grouting efficiency is proposed, which can provide a new idea for considering the settlement in grouting process. The variation of grouting efficiency can be evaluated more accurately and it is significant to the application of compensation grouting to mitigate the settlement caused by tunnel excavation.

However, the proposed approach cannot be used in all compaction grouting and can only be adopted in the situation when it's aimed at compensating the surface settlement. Meanwhile, due to the various assumptions, for example, the variation of some parameters in grouting, like porosity n and permeability coefficient k, are not considered and the grout is not complete Newton fluid in actual situations, there is some deviation between calculated grouting efficiency and actual grouting efficiency, which is necessary to do further researched and discussions.

Acknowledgments

This work was supported by Guizhou Provincial Science and Technology Major Project, No. Qian-ke-he-zhong-da-zhuan-xiang-zi [2018]3010.

References

Au, S.K.A. (2001), "Fundamental study of compensation grouting in clay.", Ph.D. Thesis, University of Cambridge, Cambridge, U.K.

Au, S.K.A., Bolton, M.D. and Soga, K. (2002), "Effect of multiple injection on long-term compensation grouting - laboratory and numerical studies", *Proceedings of the 3rd International Symposiu, On Geotechnical Aspects of Underground Construction in Soft Ground*, Specifique, Lyon, France.

Au, S.K.A., Soga, K., Jafari, M.R., Bolton, M.D. and Komiya, K. (2003), "Factors affecting long-term efficiency of compensation grouting in clays", *J. Geotech. Geoenviron. Eng.*, **129**(3), 254-262. https://doi.org/10.1061/(ASCE)1090-0241(2003)129:3(254).

Bellendir, E.N., Aleksandrov, A.V., Zertsalov, M.G. and Simutin, A.N. (2016), "Building and structure protection and leveling using compensation grouting technology", *Power Technol. Eng.*, **50**(2), 142-146. http://dx.doi.org/10.1007%2Fs10749-016-0674-y.

Bezuijen, A., Grotenhuis, R.T., Tol, A.F.V., Bosch, J.W. and Haasnoot, J.K. (2008), "Analytical model for fracture grouting in sand", *J. Geotech. Geoenviron. Eng.*, **137**(6), 611-620. https://doi.org/10.1061/(ASCE)GT.1943-5606.0000465.

Bezuijen, A., Sanders, M.P.M., Den, D., Geodelft, H. and Tol, A.F.V. (2007), "Laboratory tests on compensation grouting, the influence of grout bleeding", *Proceedings of the 33rd ITA-AITES World Tunnel Congress*, Prgaue, Czech Republic, May.

Bai, R.B., Zheng, G., Diao, Y., Du, Y.M. and Cheng, X.S. (2018), "Experimental study and numerical analysis of tunnel deformation control by compensation grouting", *China Harbour Eng.*, **38**(3), 24-29.

Chen, G.H., Zou, J.F. and Chen, J.Q. (2019c), "Shallow tunnel face stability considering pore water pressure in non-homogeneous and anisotropic soils", *Comput. Geotech.*, **116**, 103205. https://doi.org/10.1016/j.compgeo.2019.103205.

Chen, G.H., Zou, J.F. and Qian, Z.H. (2019a), "An improved collapse analysis mechanism for the face stability of shield tunnel in layered soils", *Geomech. Eng.*, **17**(1), 97-107. https://doi.org/10.12989/gae.2019.17.1.097.

Chen, G.H., Zou, J.F., Min, Q., Guo, W.J. and Zhang, T.Z. (2019b), "Face stability analysis of a shallow square tunnel in non-homogeneous soils", *Comput. Geotech.*, **114**, 103112. https://doi.org/10.1016/j.compgeo.2019.103112.

Chen, R.P., Tang, L.J., Yin, X.S., Chen, Y.M. and Bian, X.C. (2015), "An improved 3D wedge-prism model for the face stability analysis of the shield tunnel in cohesionless soils", *Acta Geotech.*, **10**(5), 683-692. https://doi.org/10.1007/s11440-014-0304-5.

Dan, H. C., Zhang, Z., Liu, X. and Chen, J.Q. (2017), "Transient unsaturated flow in the drainage layer of a highway: Solution and drainage performance", *Road Mater. Pavement Des.*, **20**(3), 528-553. https://doi.org/10.1080/14680629.2017.1397049.

Dan, H.C., He, L.H. and Zhao, L.H. (2018), "Experimental investigation on the resilient response of unbound graded aggregate materials by using large-scale dynamic triaxial tests", *Road Mater. Pavement Des.*, **21**(2), 434-451. https://doi.org/10.1080/14680629.2018.1500300.

Eisa, K. (2008), "Compensation grouting in sand", Ph.D. Dissertation, University of Cambridge, Cambridge, U.K.

El-Kelesh, A.M., Mossaad, M.E. and Basha, I.M. (2001), "Model of compaction grouting", *J. Geotech. Geoenviron. Eng.*, **127**(11), 955-964.

https://doi.org/10.1061/(ASCE)1090-0241(2001)127:11(955).

Fan, G., Zhong, D., Yan, F. and Yue, P. (2016), "A hybrid fuzzy evaluation method for curtain grouting efficiency assessment based on an AHP method extended by D numbers", *Expert Syst. Appl.*, **44**(C), 289-303. https://doi.org/10.1016/j.eswa.2015.09.006.

Gustin E.J.G., Karim, U.F.A. and Brouwers, H.J.H. (2007), "Bleeding characteristics for viscous cement and cement-bentonite grouts", *Géotechnique*, **57**(57), 391-395. https://doi.org/10.1680/geot.2007.57.4.391.

Huang F., Zhang M., Wang F., Ling T.H. and Yang X.L. (2020), "The failure mechanism of surrounding rock around an existing shield tunnel induced by an adjacent excavation", *Comput. Geotech.*, **117**, 103236. https://doi.org/10.1016/j.compgeo.2019.103236.

Ibrahim, E., Soubra, A.H. and Mollon, G. (2015), "Three-dimensional face stability analysis of pressurized tunnels driven in a multilayered purely frictional medium", *Tunn. Undergr. Sp. Technol.*, **49**(1), 18-34. https://doi.org/10.1016/j.tust.2015.04.001.

Kim, D. and Park, K. (2017), "Evaluation of the grouting in the sandy ground using bio injection material", *Geomech. Eng.*, **12**(5), 739-752. https://doi.org/10.12989/gae.2017.12.5.739.

Lee, H.B., Oh, T.M., Park, E.S., Lee, J.W. and Kim, H.M. (2017), "Factors affecting waterproof efficiency of grouting in single rock fracture", *Geomech. Eng.*, **12**(5), 771-783. https://doi.org/10.12989/gae.2017.12.5.771.

Li, C. and Zou, J.F. (2019), "Anisotropic elasto-plastic solutions for cavity expansion problem in saturated soil mass", *Soils Found.*, **59**(5), 1313-1323. https://doi.org/10.1016/j.sandf.2019.05.012.

Li, C., Zou, J.F. and Li, L. (2020), "A novel approach for predicting lateral displacement caused by pile installation", *Geomech. Eng.*, **20**(2), 147-154. https://doi.org/10.12989/gae.2020.20.2.147.

Li, C., Zou, J.F. and Si-ga, A. (2019), "Closed-Form solution for undrained cavity expansion in anisotropic soil mass based on spatially mobilized plane failure criterion", *Int. J. Geomech.*, **19**(7), 04019075. https://doi.org/10.1061/(ASCE)GM.1943-5622.0001458.

Li, T.Z. and Yang, X.L. (2020), "Stability of plane strain tunnel headings in soils with tensile strength cut-off", *Tunn. Undergr. Sp. Technol.*, **95**, 103138. https://doi.org/10.1016/j.tust.2019.103138.

Mair, R.J., Rankin, W.J., Essler, R.D. and Chipp, P.N. (1994), "Compensation grouting", *Int. J. Rock Mech. Min. Sci. Geomech. Abstr.*, **7**(1), 39-41.

Masini, L. (2010), "Studio sperimentale della tecnica delle iniezioni di compensazione in terreni sabbiosi e limosi", Ph.D. Thesis, Sapienza University of Rome, Rome, Italy (in Italian).

Masini, L., Rampello, S. and Soga, K. (2014), "An approach to evaluate the efficiency of compensation grouting", *J. Geotech. Geoenviron. Eng.*, **140**(12), 04014073. https://doi.org/10.1061/(ASCE)GT.1943-5606.0001180.

Masini, L., Rampello, S., Viggiani, G. and Soga, K. (2011), "Experimental and numerical study of group injections in silty soils", *Proceedings of the 7th International Symposium on Geotechnical Aspects of Underground Construction in Soft Ground*, Rome, Italy, May.

Merkin, V., Konyukhov, D., Simutin, A. and Medvedev, G. (2016), "Stabilizing of high-altitude position of the centrifuge foundation by compensation grouting technique during underground tunneling", *Procedia Eng.*, **165**, 658-662. https://doi.org/10.1016/j.proeng.2016.11.763.

Pan, Q. and Dias, D. (2017), "Upper-bound analysis on the face stability of a non-circular tunnel", *Tunn. Undergr. Sp. Technol.*, **62**, 96-102. https://doi.org/10.1016/j.tust.2016.11.010.

Pan, Q. and Dias, D. (2018), "Three dimensional face stability of a tunnel in weak rock masses subjected to seepage forces", *Tunn. Undergr. Sp. Technol.*, **71**, 555-566. https://doi.org/10.1016/j.tust.2017.11.003.

Qian, Z.H., Zou, J.F., Jie, T. and Pan, Q.J. (2020), "Estimations of active and passive earth thrusts of non-homogeneous frictional soils using a discretisation technique", *Comput. Geotech.*, **119**(3), 103366. https://doi.org/10.1016/j.compgeo.2019.103366.

Sanders, M.P.M. (2007), "Hydraulic fracture grouting, laboratory test in sand", Ph.D. Dissertation, Delft University of Technology, Delft, The Netherlands.

Si, K.A. (2001), "Fundamental study of compensation grouting in clay", Ph.D. Dissertation, University of Cambridge, Cambridge, U.K.

Soga, K., Au, S.K A., Jafari, M.R. and Bolton, M.D. (2004), "Laboratory investigation of multiple grout injections into clay", *Géotechnique*, **54**(2), 81-90.

Soga, K., Bezuijen, A. and Eisa, K. (2012), "The efficiency of compensation grouting in sands", *Proceedings of the 7th International Symposium on Geotechnical Aspects of Underground Construction in Soft Ground*, Rome, Italy, May.

Stärk, A., Pujol, R.S., Hill, N. and Kettle, C.T. (2017), "Compensation grouting - Balance between asset protection and collateral damage through the example of Crossrail C510", *Geomech. Tunn.*, **10**(5), 489-496. https://doi.org/10.1002/geot.201700034.

Taylor, D.W. (1948), *Fundamentals of Soil Mechanics*, in *Soil Science*, Wolters Kluwer.

Ukritchon, B., Yingchaloenkitkhajorn, K. and Keawsawasvong, S. (2017), "Three-dimensional undrained tunnel face stability in clay with a linearly increasing shear strength with depth", *Comput. Geotech.*, **88**, 146-151. https://doi.org/10.1016/j.compgeo.2017.03.013.

Zhang, C., Han, K. and Zhang, D. (2015), "Face stability analysis of shallow circular tunnels in cohesive–frictional soils", *Tunn. Undergr. Sp. Technol.*, **50**, 345-357. https://doi.org/10.1016/j.tust.2015.08.007.

Zhang, J., Li, S.C., Li, L.P., Zhang, Q.Q, Xu, Z.H, Wu, J. and He, P. (2017), "Grouting effects evaluation of water-rich faults and its engineering application in Qingdao Jiaozhou Bay Subsea Tunnel, China", *Geomech. Eng.*, **12**(1), 35-52. https://doi.org/10.12989/gae.2017.12.1.035.

Zheng, G., Zhang, X.S., Diao, Y. and Lei, H.Y. (2016), "Experimental study on the performance of compensation grouting in structured soil", *Geomech. Eng.*, **10**(3), 335-355. https://doi.org/10.12989/gae.2016.10.3.335.

Zou, J. F., Yang, T., Ling, W., Guo, W. and Huang, F. (2019a), "A numerical stepwise approach for cavity expansion problem in strain-softening rock or soil mass", *Geomech. Eng.*, **18**(3), 225-234. https://doi.org/10.12989/gae.2019.18.3.225.

Zou, J.F. and Zhang, P.H. (2019), "Analytical model of fully grouted bolts in pull-out tests and in situ rock masses", *Int. J. Rock Mech. Min. Sci.*, **113**(1), 278-294. https://doi.org/10.1016/j.ijrmms.2018.11.015.

Zou, J.F. and Zuo, S.Q. (2017), "Similarity solution for the synchronous grouting of shield tunnel under the vertical non-axisymmetric displacement boundary condition", *Adv. Appl. Math. Mech.*, **9**(1), 205-232. https://doi.org/10.4208/aamm.2016.m1479.

Zou, J.F., Chen, G.H. and Qian, Z.H. (2019b), "Tunnel face stability in cohesion-frictional soils considering the soil arching effect by improved failure models", *Comput. Geotech.*, **106**(2), 1-17. https://doi.org/10.1016/j.compgeo.2018.10.014.

Zou, J.F., Liu, S.X., Li, J.B. and Qian, Z.H. (2019c), "Face stability analysis for a shield-driven tunnel with non-linear yield criterion", *Proc. Inst. Civ. Eng. Geotech. Eng.*, **172**(3), 243-254.

https://doi.org/10.1680/jgeen.17.00222.
Zou, J.F., Sheng, Y.M. and Xia, M.Y. (2020), "A novel numerical-iterative-approach for strain-softening surrounding rock incorporating rockbolts effectiveness and hydraulic-mechanical coupling based on Three-Dimensional Hoek-Brown strength criterion", *Tunn. Undergr. Sp. Technol.*, In Press.
Zou, J.F., Wei, A. and Li, L. (2020), "Analytical solution for steady seepage and groundwat inflow into an underwater tunnel", *Geomech. Eng.*, **20**(3), 267-273. https://doi.org/10.12989/gae.2020.20.3.267.
Zou, J.F., Wei, A. and Yang, T. (2018), "Elasto-plastic solution for shallow tunnel in semi-infinite space", *Appl. Math. Modell.*, **64**(12), 669-687. https://doi.org/10.1016/j.apm.2018.07.049.

CC

Notations

ξ	compensation grouting efficiency
η_G	geometry effect
η_S	soil compaction/consolidation
η_F	the grout filtration effect
V_{SH}	volume of heave induced at the ground surface by the injection process
V_{inj}	volume of injected grout
V_{GB}	volume of the grout body
$V_{GB\text{-}final}$	final volume of the grout body
V_S	increased soil volume due to grouting
$V_{w\text{-}out}$	volume of fluid lost by pressure filtration
V_{fg}	volume of filtered grout
n_g, n_{fg}	porosity of slurry grout and filtered grout, respectively
Q	flow rate of pore water moving outward in the filtered grout
p_{inj}	injection pressure
t	grouting time
γ_w	unit weight of water
r	distance where pore pressure can be negligible
k	permeability coefficient
r_i	radius of grout body at time t
k_g, k_{fg}, ks	permeability coefficient of slurry grout, filtered grout and soil, respectively
L_{fg}	thickness of filtered grout at time t
a_0	drilling radius or initial cavity radius
a_1, a_2, a_3, a_4, a_5	constants depending on the soil type and injection depth
q	initial isotropic ground stress
I_r	stiffness coefficient
R_u	ultimate radius of grout bulb
E	elastic modulus
c	cohesion of soil
φ	friction angle
v	Poisson ratio
q_{inj}	injection rate